Journal of Power Sources 264 (2014) 123–127

Contents lists available at ScienceDirect

Journal of Power Sources

journal homepage: www.elsevier.com/locate/jpowsour

Short communication

A novel lithium vanadium fluorophosphate nanosheet with uniform carbon coating as a cathode material for lithium-ion batteries

Bao Zhang, Ya-dong Han, Jun-chao Zheng*, Chao Shen, Lei Ming, Jia-feng Zhang

School of Metallurgy and Environment, Central South University, Changsha 410083, PR China

HIGHLIGHTS

- High-purity $LiVPO_4F$ nanosheets were prepared for the first time.
- Each $LiVPO_4F$ nanosheet had a typical thickness of 50–100 nm.
- Each $LiVPO_4F$ nanosheet had a uniform carbon coating.
- $LiVPO_4F$ nanosheets deliver an excellent electrochemical performance.

ARTICLE INFO

Article history:
Received 23 January 2014
Received in revised form
2 April 2014
Accepted 21 April 2014
Available online 28 April 2014

Keywords:
Lithium-ion battery
Cathode material
Lithium vanadium fluorophosphates
Nanosheet
Electrochemical performance

ABSTRACT

Lithium vanadium fluorophosphate ($LiVPO_4F/C$) nanosheets with uniform carbon coating are successfully synthesized using a hydrothermal method followed by calcination. X-ray diffraction results reveal that the obtained products crystallized in the triclinic $LiVPO_4F$ phase. Scanning electron microscope and transmission electron microscope images demonstrate that both vanadium phosphate (VPO_4/C) and $LiVPO_4F/C$ composites have a very flat sheet-like morphology, with each nanosheet exhibiting a smooth surface and a typical thickness of 50–100 nm. The nanosheets are coated by a uniform layer of amorphous carbon. Electrochemical tests show that $LiVPO_4F$ nanosheets deliver a discharge capacity of 143 mAh g^{-1} at 0.1 C in the range of 3.0–4.5 V at the first cycle and possess a favorable capacity at rates of 0.5, 1, 2, 3 and 5 C.

1. Introduction

Lithium vanadium fluorophosphate ($LiVPO_4F$), a novel 4 V cathode material with a theoretical capacity of 156 mAh g^{-1}, was reported by Barker et al., in 2003 [1]. Considering its excellent rate capability, long cycle life, safety, high-energy density, and high voltage in lithium-ion cells, $LiVPO_4F$ is a potential alternative to the commonly used $LiCoO_2$ [1–6]. $LiVPO_4F$ is usually synthesized through conventional one or two-step solid reactions [1–4,7–10], the sol–gel method [11,12], or chemical lithiation and post-annealing [13,14]. Results indicate, however, that high-purity $LiVPO_4F$ samples are very difficult to obtain [6,7,10,12–14]. High-purity is a crucial element influencing electrochemical performance and cyclic stability [11,15]. Moreover, the electronic conductivity of $LiVPO_4F$ is low, although better than that of traditional phosphates, such as $LiFePO_4$, $LiMnPO_4$ and $LiVOPO_4$ [16]. Thus, exploration of novel synthesis approaches to overcome the difficulties described above is needed. In the present work, the synthesis of high-purity $LiVPO_4F/C$ nanosheets with a uniform carbon coating using a novel hydrothermal method is presented, and the properties of these nanosheets are investigated.

2. Experimental

VPO_4 nanosheets were prepared through a hydrothermal method. Stoichiometric amounts of V_2O_5 (AR, ≥99.0%), $NH_4H_2PO_4$ (AR, ≥99.0%), and citrate (AR, ≥99.0%) were mixed in deionized water with continuous stirring under 80 °C for 2 h. The pH of the solution was adjusted to 7 using ammonia water. The mixed solution was then transferred into a 100 mL Teflon vessel, sealed in an autoclave, and hydrothermally treated at 250 °C for 20 h. A yellow precipitate was obtained. The amorphous V-PO_4 precursor was washed in deionized water several times and dried in an oven at 80 °C. The synthesis of amorphous V-PO_4/C composites is schematically illustrated in Fig. 1.

* Corresponding author. Tel.: +86 731 88836357.
E-mail addresses: jczheng@csu.edu.cn, tonyson_011@163.com (J.-c. Zheng).

http://dx.doi.org/10.1016/j.jpowsour.2014.04.087
0378-7753/

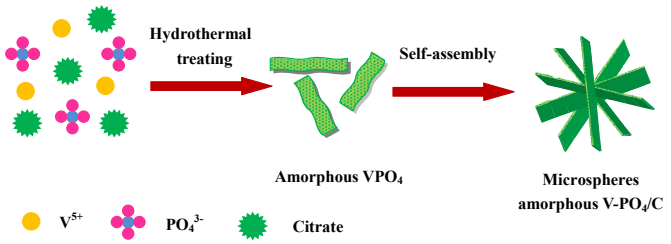

Fig. 1. Schematic illustration of synthesis process for amorphous V-PO_4/C.

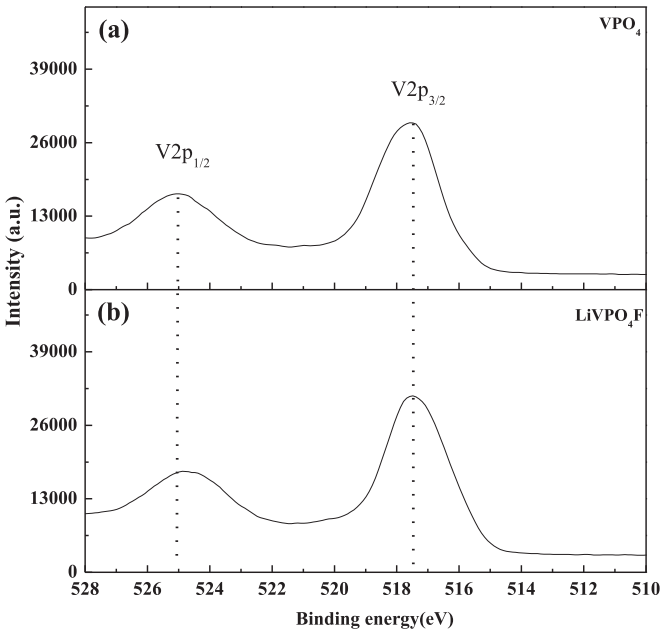

Fig. 2. XPS spectra of V2p for (a) VPO_4/C; (b) $LiVPO_4F$/C.

To prepare $LiVPO_4F$ nanosheets, stoichiometric amounts of VPO_4 (annealed at 725 °C for 4 h under an Ar atmosphere before mixing with other components) and LiF (AR, ≥99.0%) were mixed in an agate mortar and subsequently heated at 625 °C for 30 min under an Ar atmosphere. $LiVPO_4F$/C nanosheets were finally obtained.

Powder X-ray diffraction (XRD) (Rint-2000, Rigaku) measurement using Cu Kα radiation was utilized to identify the crystalline phases of the synthesized materials. The valence state of vanadium in the prepared precursor was determined using an X-ray photoelectron spectrometer (XPS, Kratos Model XSAM800) equipped with a Mg Kα achromatic X-ray source (1235.6 eV). The samples were observed using a scanning electron microscope (SEM; JEOL, JSM-5600LV) and a Tecnai G12 transmission electron microscope (TEM). Elemental carbon analysis was performed using C–S analysis equipment (Eltar, Germany). Sample contents were analyzed by inductively coupled plasma emission spectroscopy (ICP, IRIS Intrepid XSP, Thermo Electron Corporation).

Electrochemical characterization was performed using a CR2025 coin-type cell. Typical positive electrode loadings ranged from 2 mg cm^{-2} to 2.5 mg cm^{-2}, and an electrode with a diameter of 14 mm was used. For positive electrode fabrication, the prepared powders were mixed with 10% carbon black and 10% polyvinylidene fluoride in *N*-methyl pyrrolidinone until a slurry was obtained. The blended slurries were then pasted onto an aluminum current collector, and the electrode was dried at 120 °C for 12 h in Ar. The test cell consisted of the positive electrode and a lithium foil negative electrode separated using a porous polypropylene film and 1 mol L^{-1} $LiPF_6$ in EC, EMC, and DMC (1:1:1 v/v/v) as the electrolyte. Cell assembly was carried out in a dry Ar-filled glove box. Electrochemical tests were conducted using an automatic galvanostatic charge–discharge unit and NEWARE battery cycler. Cyclic voltammetric measurements were performed with a CHI660D electrochemical analyzer.

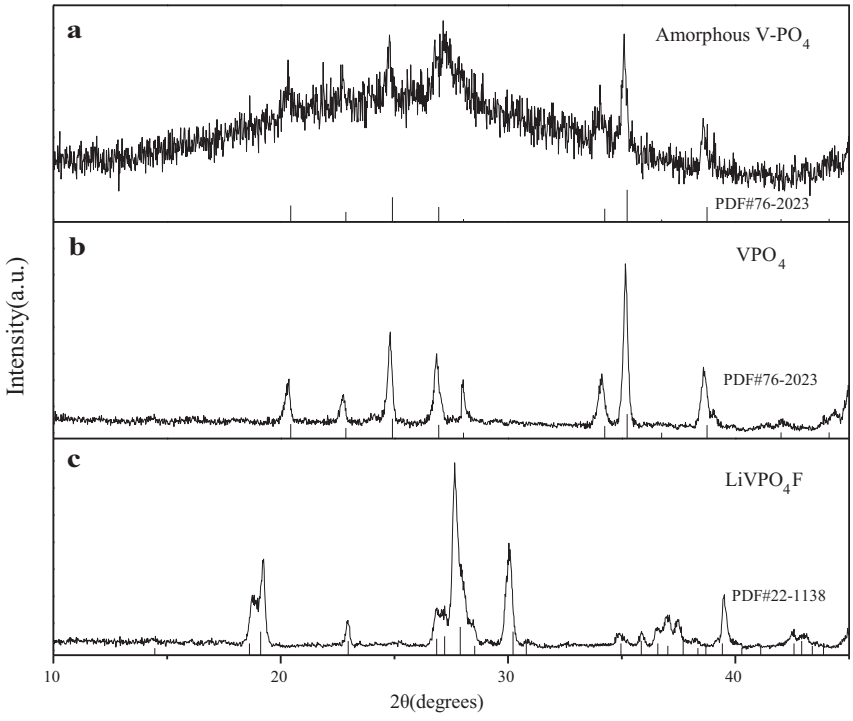

Fig. 3. XRD patterns for (a) amorphous V-PO_4/C; (b) VPO_4/C; (c) $LiVPO_4F$/C.

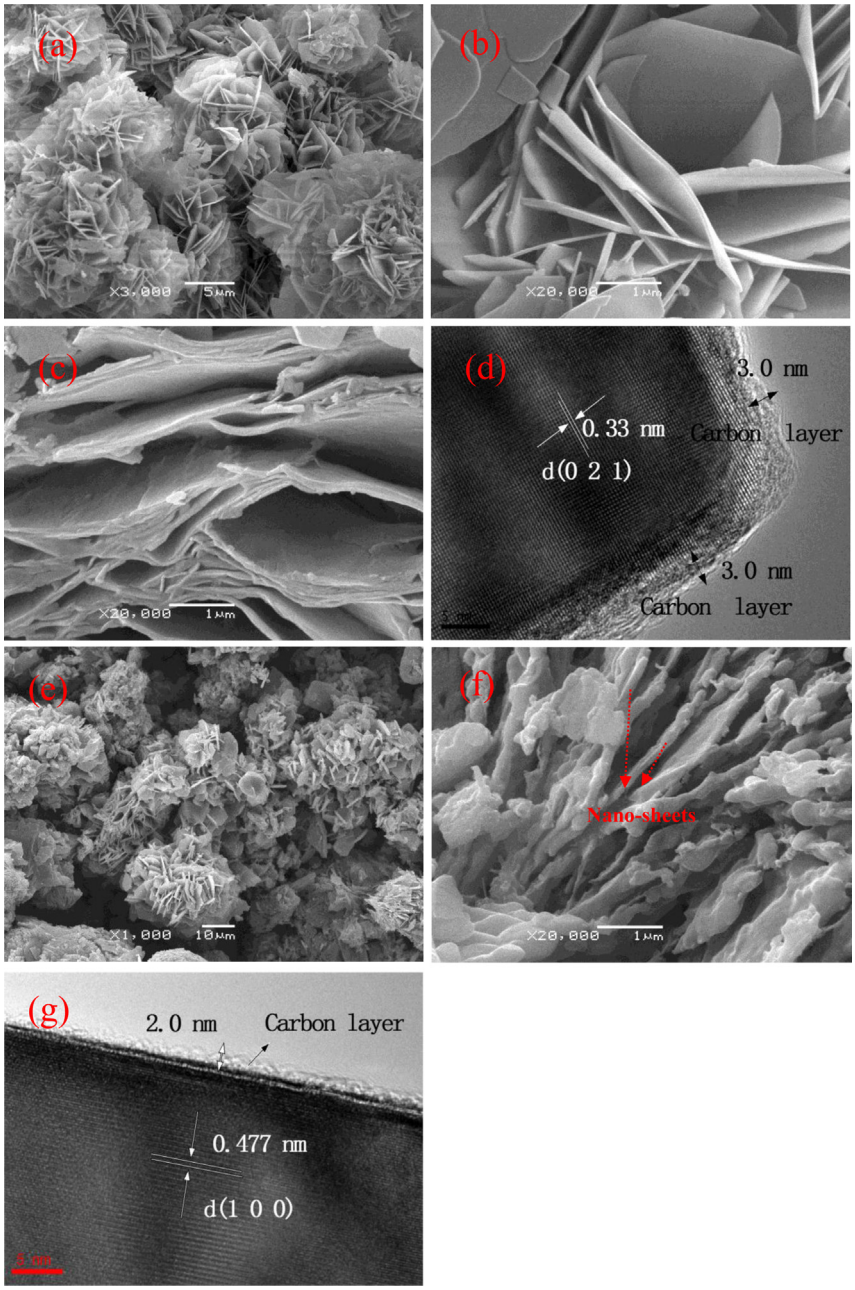

Fig. 4. (a), (b) SEM images of amorphous V-PO_4/C; (c) SEM image of VPO_4/C; (d) TEM image of VPO_4/C; (e), (f) SEM image of $LiVPO_4F$/C; (g) TEM image of $LiVPO_4F$/C.

3. Results and discussion

The vanadium/phosphate (V/P) molar ratio of the dried yellow solid at 80 °C is 1.01, as determined by ICP, which confirms the stoichiometry of V/P species. XPS spectra of the V-PO_4 precursor and synthesized $LiVPO_4F$ samples are illustrated in Fig. 2. The binding energy (BE) values of V2p in the V-PO_4 precursor (synthesized $LiVPO_4F$) are 517.3 (517.3) eV and 524.8 (524.7) eV, corresponding to the energy levels $V2p_{3/2}$ and $V2p_{1/2}$, respectively (Fig. 2). Spin orbit coupling induces V2p to split [6]. The BE of $V2p_{3/2}$ of the samples matches values observed in $LiVPO_4F$ (517.0 eV) [13] and V_2O_3 (517.3 eV) [21] well; this finding indicates that the oxidation state of vanadium is +3.

Fig. 3a shows the XRD pattern of a sample hydrothermally heated at 250 °C for 20 h. No diffraction peaks are present in Fig. 3a, which indicates that the synthesized sample is amorphous. After calcination at about 725 °C for 4 h, the compound shows a series of diffraction peaks in its XRD pattern, as shown in Fig. 3b. The crystal structure is identified to be monoclinic VPO_4 structure, consistent with a previous report [17]. The XRD pattern of the synthesized $LiVPO_4F$ sample is shown in Fig. 3c; all of the peaks can be indexed to a triclinic structure. No diffraction peaks were identified as LiF, $Li_3V_2(PO_4)_3$, or other impurities, which indicates that the synthesized $LiVPO_4F$ is pure. These results are better than those previously reported [6,7,10–14]. The amounts of carbon in the VPO_4/C and $LiVPO_4F$/C samples are 4.78 and 3.97 wt%, respectively, as determined by C–S analysis. The carbon in the composite was not detected by XRD, which indicates that the residual carbon is amorphous.

Fig. 4a and b shows SEM images of the amorphous V-PO_4. The amorphous V-PO_4 microspheres are made of nanosheets with

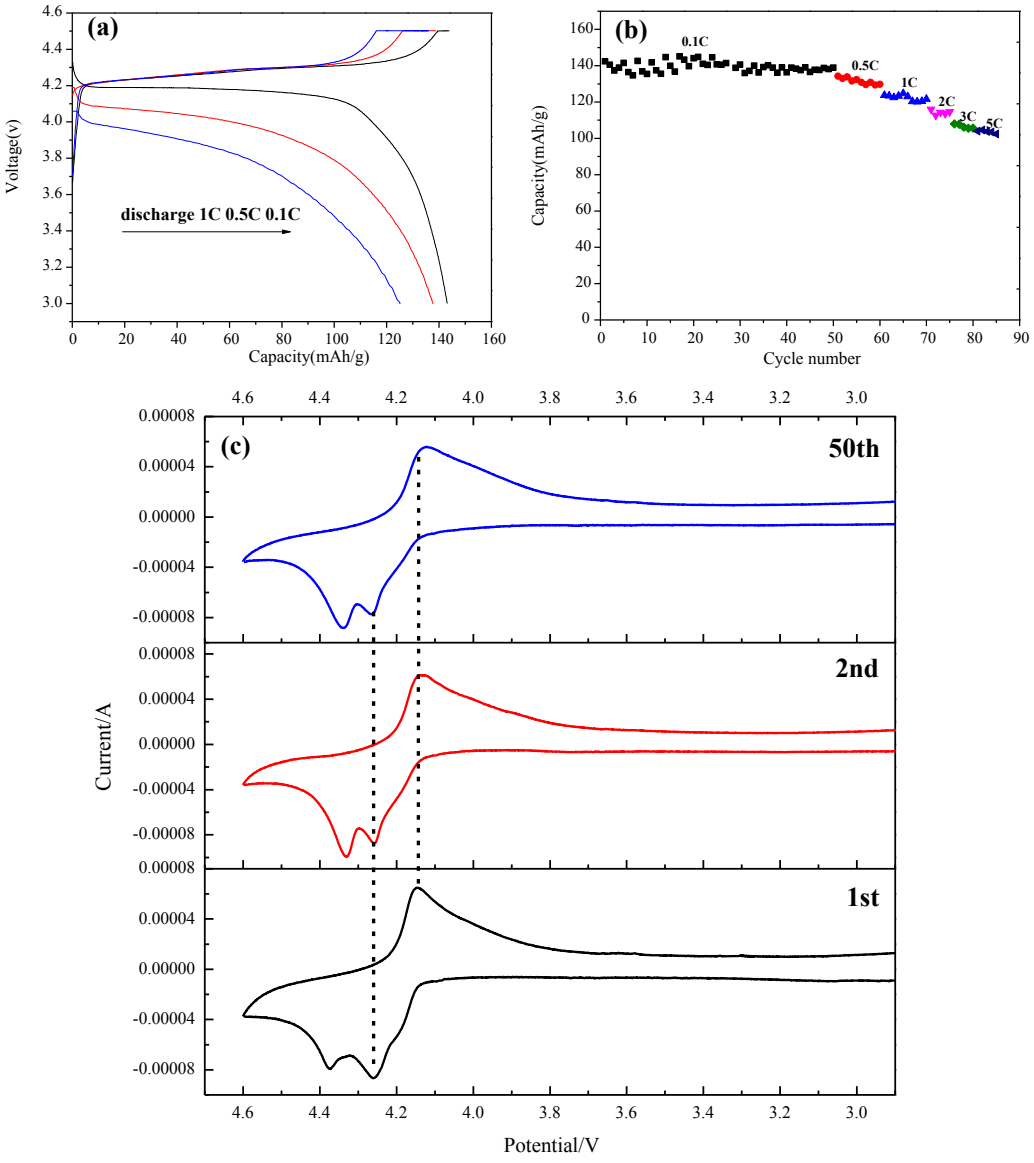

Fig. 5. (a) Charge/discharge performance of $LiVPO_4F$ at different rate; (b) cycle performance of $LiVPO_4F$ at 0.1 C, 0.5 C, 1 C, 2C, 3 C, 5 C; (c) cyclic voltammogram recorded for $LiVPO_4F$ at a scan rate of 0.1 mV s^{-1}.

thicknesses ranging from 50 nm to 100 nm (Fig. 4b). Fig. 4c and d shows SEM and TEM images, respectively, of VPO_4/C calcined at 725 °C for 4 h. The sample maintains the nanosheet shape, and the staggered nanosheets are uniformly encapsulated in the carbon shell with a thickness of about 3 nm. The lattice fringe of VPO_4 with an interplanar spacing of 0.33 nm corresponds to the (0 2 1) lattice plane. Fig. 4e to g show the SEM and TEM images of the synthesized $LiVPO_4F$, which also maintains the shape of nanosheets. The $LiVPO_4F$ nanosheets obtained are not agglomerated, and interspaces between the sheets are preserved. The nanosheet surfaces are coated by a uniform carbon layer with a thickness of about 2 nm. Crystal planes with a *d*-spacing of 0.477 nm correspond to the (1 0 0) plane of triclinic $LiVPO_4F$.

Nanomaterials provide short diffusion pathways for lithium-ion insertion or extraction from host materials, large specific surface areas can afford more active intercalation sites [18–20]. The $LiVPO_4F$ nanosheets not only shorten the transport path of Li^+ but also increase the electrode and electrolyte contact areas, which may result in excellent electrochemical performance.

Fig. 5a shows the charge/discharge curves of Li/$LiVPO_4F$ cells at different rates. The initial discharge capacity is 143.1 mAh g^{-1} with a plateau at 4.17 V vs. Li/Li^+ and 0.1 C, which is about 91.6% of the theoretical capacity (156 mAh g^{-1}). The discharge capacity is maintained at 138.9 mAh g^{-1} after 50 cycles, which is about 97.06% of its initial discharge capacity, as shown in Fig. 5b. At higher discharge rates of 0.5, 1, 2, 3, and 5 C, the cell delivers a capacity of 137.6, 124.7, 116.6, 107.9, and 104.2 mAh g^{-1}, respectively. The electrochemical performance of the prepared $LiVPO_4F$ is better than that reported by other researchers, as seen in Table 1. This excellent electrochemical performance is attributed to the nanosheet morphology of $LiVPO_4F$, which can provide more active sites, short diffusion distances, and good contact between the active material and electrolyte. The unique nanostructure and uniform carbon coating of the material facilitate effective lithium insertion and extraction. No other plateaus are observed in the charge/discharge curves. The current findings are consistent with the XRD measurements but different from results previously reported [6,7,9,12–14].

Table 1
Comparison on electrochemical properties of $LiVPO_4F$/C in this work and that in other reports.

Samples	Initial discharge capacity (mAh g^{-1})	Discharge capacity (mAh g^{-1})	Cyclic performance (mAh g^{-1})
LVPF in Ref. [6]	123 at 0.12 C	106 at 0.92 C	121 at 0.1 C after 12 cycles
LVPF in Ref. [7]	132 at 0.1 C	118 at 1 C	124 at 0.1 C after 50 cycles
LVPF in Ref. [11]	130.6 at 0.1 C	–	124 at 0.1 C after 30 cycles
LVPF in Ref. [12]	134 at 0.1 C	127 at 1 C	125 at 0.1 C after 30 cycles
LVPF in this work	141.3 at 0.1 C	124.7 at 1 C	138.9 at 0.1 C after 50 cycles

Cyclic voltammograms were recorded with Li metal as the counter and reference electrodes in the voltage range of 3.0–4.6 V at a scan rate of 0.1 mV s^{-1} and room temperature, as shown in Fig. 5c. Redox peaks for $Li_{1-x}VPO_4F$ (4.25 and 4.35 V for oxidation peaks, and 4.17 V for the reduction peak) with slight polarization are observed in the 1st, 2nd, and 50th curves, consistent with the charge/discharge tests. Fig. 5c shows that the positions of redox peaks change minimally after 50 cycles, indicating slight polarization and good cycling performance. Two peaks may be attributed to deintercalation of $Li_{1-x}VPO_4F$, while one peak is attributed to its intercalation. Extraction from two different Li^+ sites requires different energies, but all Li^+ cations tend to take over only one Li^+ site during insertion. This insertion process is identical to that previously reported in the literature [1,7].

4. Conclusions

High-purity $LiVPO_4F$/C was synthesized *via* a hydrothermal method followed by calcination. SEM and TEM images demonstrate that VPO_4/C and $LiVPO_4F$/C microspheres are composed of nanosheets with a uniform carbon coating. Electrochemical tests showed that $LiVPO_4F$ nanosheets deliver excellent electrochemical performance, which was attributed to the unique nanostructure and uniform carbon coating of the material. Synthesizing high-purity $LiVPO_4F$/C nanosheets with a uniform carbon coating presents a novel method for improving the electrochemical performance of batteries.

Acknowledgment

This study was supported by National Natural Science Foundation of China (Grant no. 51302324).

References

[1] J. Barker, M.Y. Saidi, J.L. Swoyer, J. Electrochem. Soc. 150 (2003) A684–A688.
[2] J. Barker, M.Y. Saidi, J.L. Swoyer, J. Electrochem. Soc. 151 (2004) A1670–A1677.
[3] J. Barker, R.K.B. Gover, P. Burns, A. Bryan, Electrochem. Solid-State Lett. 8 (2005) A285–A287.
[4] J. Barker, R.K.B. Gover, P. Burns, A. Bryan, M.Y. Saidi, J.L. Swoyer, J. Electrochem. Soc. 152 (2005) A1776–A1779.
[5] R.K.B. Gover, P. Burns, A. Bryan, M.Y. Saidi, J.L. Swoyer, J. Barker, Solid State Ionics 177 (2006) 2635–2638.
[6] M.V. Reddy, G.V. Subba Rao, B.V.R. Chowdari, J. Power Sources 195 (2010) 5768–5774.
[7] Q. Zhang, S. Zhong, L. Liu, J. Jiang, J. Wang, Y. Li, J. Phys. Chem. Solids 70 (2009) 1080–1082.
[8] H. Huang, T.J. Faulkner, ECS Trans. 33 (2011) 239–243.
[9] F. Zhou, X. Zhao, J.R. Dahn, Electrochem. Commun. 11 (2009) 589–591.
[10] R. Ma, J. Shu, L. Hou, M. Shui, L. Shao, D. Wang, Y. Ren, Ionics 19 (2013) 1–6.
[11] Y. Li, Z. Zhou, X.P. Gao, J. Yan, J. Power Sources 160 (2006) 633–637.
[12] S.-k. Zhong, W. Chen, Y.-h. Li, Z.-g. Zou, C.-j. Liu, Trans. Nonferrous Met. Soc. China 20 (2010) s275–s278.
[13] J.-c. Zheng, B. Zhang, Z-h. Yang, J. Power Sources 202 (2012) 380–383.
[14] J. Wang, X. Li, Z. Wang, et al., Electrochim. Acta 91 (2013) 75–81.
[15] Y.Z. Li, J.X. Ren, Z. Zhou, X.P. Gao, J. Yan, Chin. J. Inorg. Chem. 21 (2005) 1597–1600.
[16] J. Barker, R.K.B. Gover, P. Burns, A. Bryan, M.Y. Saidi, J.L. Swoyer, J. Power Sources 146 (2005) 516–520.
[17] J.T. Vaughey, W.T.A. Harrison, A.J. Jacobson, Inorg. Chem. 33 (1994) 2481–2487.
[18] X. Lou, D. Deng, J. Lee, et al., Adv. Mater. 20 (2008) 258–262.
[19] K.M. Shaju, F. Jiao, A. Debart, et al., Phys. Chem. Chem. Phys. 9 (2007) 1837–1842.
[20] A.S. Arico, P. Bruce, B. Scrosati, et al., Nat. Mater. 4 (2005) 366–377.
[21] J. Mendialdua, R. Casanova, Y. Barboux, J. Electron Spectrosc. Relat. Phenom. 71 (1995) 249–261.